Materials Science-Poland, 38(2), 2020, pp. 271-278
http://www.materialsscience.pwr.wroc.pl/
DOI: 10.2478/msp-2020-0032

sciendo

X-ray diffraction study of the elastic properties of jagged spherical CdS nanocrystals

PIJUSH CH. DEY, SUMIT SARKAR, RATAN DAS*

Nano-Physics & Nanotechnology Research Lab., Department of Physics, Tripura University (A Central University), Suryamaninagar, Tripura-799022, India

In this work, jagged spherical CdS nanocrystals have been synthesized by chemical method to study their elastic properties. The synthesized CdS nanocrystal has been characterized by transmission electron microscopy (TEM) and X-ray diffraction (XRD). The transmission electron microscope images show that the average size of the nanocrystal is 100 nm approximately. X-ray diffraction (XRD) study confirms that the CdS nanocrystals are in cubic zinc blende structure. The size calculated from the XRD is consistent with the average size obtained from the TEM analysis. The XRD data have been analyzed to study the elastic properties of the jagged spherical CdS nanocrystals, such as intrinsic strain, stress and energy density, using Williamson-Hall plot method. Williamson-Hall method and size-strain plot (SSP) have been used to study the individual effect of crystalline size and lattice strain on the peak broadening of the jagged spherical CdS nanocrystals. Size-strain plot (SSP) and root mean square (RMS) strain further confirm the results obtained from W-H plots.

Keywords: *jagged spherical CdS nanocrystals; powder X-ray diffraction; elastic properties; size-strain plot; root mean square strain*

1. Introduction

Recent research on different nanosized structures has demonstrated the extraordinary optical, electrical, magnetic and mechanical properties of nanomaterials, which are different from their corresponding bulk counterparts [1–11]. In particular, semiconductor nanocrystals show excellent physical properties due to their large band gap and different defect related states [12–15]. CdS is the most promising material of II-VI group semiconductors which has a direct wide band gap of 2.42 eV at 300 K, high melting point of 1760 °C and both cubic and hexagonal structure [16, 17]. It is widely used in various applications such as light emitting devices, biosensors, solar cells and spintronics devices etc. [18–23]. There are several techniques to synthesize CdS crystals, such as, sol-gel method [24], precipitation method [25], thermal evaporation [26], chemical vapor deposition [27], hydrothermal techniques [28] etc. In this work, jagged spherical shaped CdS nanocrystals have been prepared by using chemical process to study their elastic properties. Elastic properties of nanocrystals are very important as they can affect the other properties, such as optical and electrical, because elastic properties are related to the lattice constant [29, 30], which, in turn, is related to the electron density of the nanocrystals. A change in the lattice constant, results in a change in the band gap of the nanocrystals. It has also been reported that the band gap changes with the variation of size and shape of crystals. So, lattice constant and hence elastic properties are size and shape dependent. For this reason, we have been very much interested in the study of elastic properties of jagged spherical shaped CdS nanocrystals. XRD is an important tool for the study of elastic properties of nanocrystals [31]. Structural parameters such as crystallite size, lattice planes, lattice strain and stress are analyzed by using XRD method [32].

Every crystal is imperfect due to its finite size, as a perfect crystal must extend in every direction to infinity. This imperfection in a crystal produces peak broadening in the X-ray diffraction pattern. It is well known that lattice strain and crystallite

*E-mail: dasratanphy@gmail.com

size are the two main parameters, which can be extracted from a peak width analysis. Here, the average size has been estimated by using Scherrer equation and the Scherrer plot from XRD study, which is comparable to the average size obtained from HRTEM analysis. Further, the lattice strain, stress, and the energy density of prepared CdS nanocrystals have been calculated by Williamson-Hall (W-H) analysis using different models including uniform deformation model (UDM), uniform stress deformation model (USDM) and uniform deformation energy density model (UDEDM).

2. Experimental

2.1. Synthesis of jagged spherical CdS nanocrystals

For the preparation of cadmium sulfide (CdS) nanocrystals, cadmium acetate dehydrate, thiourea, triethanolamine, ammonia solution and double distilled water have been used as the starting materials. CdS nanocrystals have been synthesized by chemical process at 40 °C [33]. In this synthesis process, cadmium acetate was used as a cadmium (Cd^{2+}) source and thiourea was used as a sulfur (S^2) source. First, 1 M cadmium acetate solution was prepared by dissolving 13 g of cadmium acetate in 50 mL of deionized water and then 15 mL of ammonia solution was added to it, preceded by 15 drops of triethanolamine (TEA). The prepared solution was continuously stirred using a magnetic stirrer at 40 °C. 1 M solution of thiourea was prepared by dissolving 3.8 g of thiourea in 50 mL of deionized water. The prepared solution of thiourea has been mixed with the previous prepared solution (cadmium acetate solution) under stirring at 40 °C. After some time, yellow colored solutions of CdS nanocrystals were formed.

2.2. Instrumentation

The crystalline structure of the CdS nanocrystals has been investigated by using Rigaku Co. Japan/Model: Miniflex X-ray diffractrometer in a standard 2θ of the Bragg diffraction with a monochromatic wavelength of CuKα radiation (λ = 0.154056 nm). The patterns of the prepared powder have been collected from XRD instrument between 20°and 60°. A HRTEM instrument (JEM-2100 transmission electron microscope with an accelerating voltage of 200 kV) was employed to study the morphology of the jagged spherical CdS nanocrystals.

3. Result and discussions

3.1. TEM analysis

Transmission electron microscope (TEM) is one of the best ways to investigate the size and shape of the prepared CdS nanocrystals. For the TEM analysis, a drop of CdS nanocrystal solution, dispersed in distilled water, was taken on the carbon coated copper grid. After evaporation, the TEM images of the CdS nanoparticles have been taken.

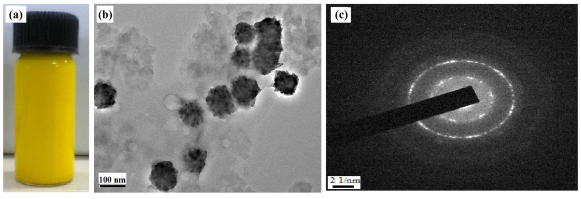

Fig. 1. (a) Synthesized CdS nanocrystals; (b) TEM images of the CdS nanocrystals; (c) SAED pattern of CdS nanocrystals.

TEM images of the CdS nanocrystals are displayed in Fig. 1b, which shows that the surface is not smooth. The corresponding SAED pattern of the prepared nanocrystals is shown in Fig. 1c. The observed morphology of the nanocrystals is found to be jagged spherical. From the TEM micrograph, the average diameter of CdS nanocrystal assemblies is found to be of 100 nm.

3.2. 3.2. X-ray diffraction analysis

The XRD pattern of the synthesized CdS nanocrystals is shown in Fig. 2.

The XRD peaks at 2θ values of 28.15°, 43.93° and 52.67° correspond to the planes of (1 1 1), (2 2 0) and (3 1 1), respectively, on matching with CPDS Card No 10-0454. Here, the instrumental broadenings at 28.15°, 43.93° and

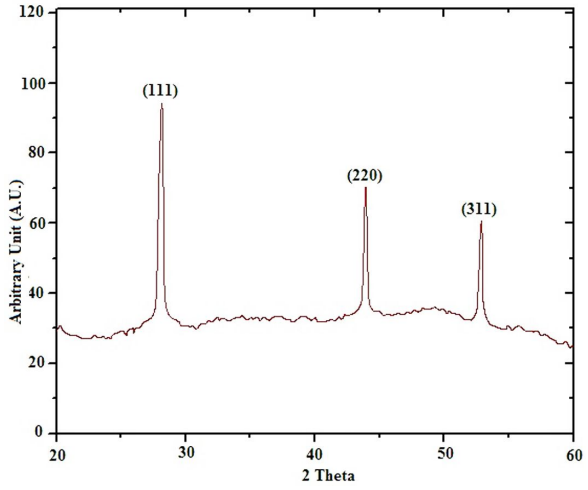

Fig. 2. XRD pattern of CdS nanocrystals.

52.67° are found as 0.00463 and 0.00632 and 0.00921, respectively, for standard silicon. In the measurement of full width at half maxima (FWHM), we considered the instrumental broadening for the respective peaks. All the peaks in the X-ray diffraction pattern indicate that the CdS nanocrystal is cubic in structure. Here, the reflection peaks from (2 0 0) and (2 2 2) are missing in the XRD spectra. The possible reason for this is the destructive interference of X-rays after reflection from these planes. Moreover, the (2 0 0) and (2 2 2) reflections in JCPDS Card No. 10-0454 have a weaker intensity of about 40 % and 10 %, respectively, which may be a reason for missing these planes. Further, when the unit cell is deformed, strained, or there are some dislocations of atoms in the cell, XRD spectra show missing planes.

3.2.1. Scherrer equation

The average crystalline size of the CdS nanocrystals can be calculated by using Scherrer equation [34–38] as:

$$D = \frac{k\lambda}{\beta_D \mathrm{Cos}\theta} \tag{1}$$

here, k is the shape factor or Scherrer constant, λ is the wavelength of X-ray line (λ = 0.154056 nm), β_D (in radians) denotes the FWHM (width of the diffraction peak) and θ (in degree) is the Bragg angle of the corresponding diffraction peak. Here, the shape is spherical and hence in equation 1, the value of the shape factor should be 1, though the surface is rough and jagged. From the above equation, the calculated average crystallite size (D) of the prepared CdS nanocrystals is 81.10 nm. Equation 1 also implies that the crystallite size is 1/cosθ dependent [39, 40].

Generally, broadening is corrected as:

$$\beta_D = \sqrt{(\beta_0)^2 - (\beta_i)^2} \tag{2a}$$

For Gaussian

$$\beta_D^2 = \beta_0^2 + \beta_i^2 \tag{2b}$$

For Lorentzian

$$\beta_D = \beta_0 + \beta_i \tag{2c}$$

where, β_i is the instrumental broadening and β_o is the experimentally observed broadening.

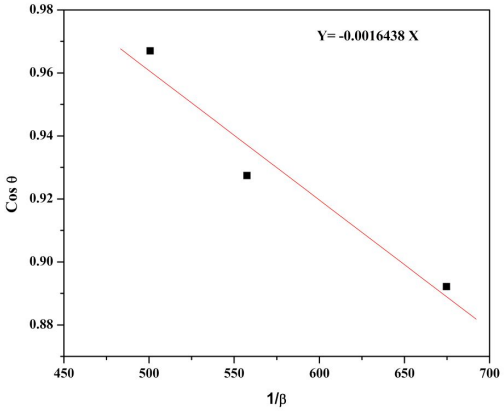

Fig. 3. Plot of cos θ vs. $1/\beta_D$.

3.2.2. Scherrer plot

Fig. 3 shows the Scherrer plot for different FWHM values with a respective cosθ value corresponding to different (h k l) planes of the XRD pattern. Plotting $1/\beta_D$ along x-direction and cosθ along y-direction, the crystallite size (D) can be calculated from the slope by linear fitting of the data as shown in Fig. 3, and the calculated value is given in Table 3. The modified Scherrer equation is given by [41]:

$$\cos\theta = \frac{k\lambda}{D}\left(\frac{1}{\beta_D}\right) \tag{3}$$

3.2.3. Williamson-Hall methods

Due to lattice imperfection and distortion, the induced strain in the nanocrystals can be calculated using Wilson formula [42] as:

$$\beta_\varepsilon = 4\varepsilon \tan\theta \tag{4}$$

The Williamson-Hall equation varies with tanθ only, instead of 1/cosθ as Debye-Scherrer equation follows [39, 40, 43]. The addition of equation 1 and equation 4 gives the observed broadening assuming the contribution of particle size and strain:

$$\beta_{hkl} = \beta_D + \beta_\varepsilon \tag{5}$$

$$\beta_{hkl} = \frac{k\lambda}{D\cos\theta} + 4\varepsilon \tan\theta \tag{6}$$

$$\beta_{hkl}\cos\theta = \frac{k\lambda}{D} + 4\varepsilon \sin\theta \tag{7}$$

Equation 7 is the Williamson-Hall equation for estimating the average crystallite size and lattice strain. In this study, the crystallite size and lattice strain of the CdS nanocrystals have been calculated by using three models such as uniform deformation model (UDM), uniform strain deformation model (USDM) and uniform energy density model (UDEDM). Equation 7 represents the uniform deformation model (UDM), which implies an isotropic nature of the materials [30, 39].

The uniform deformation model (UDM) of the CdS nanocrystals is shown in Fig. 4. The crystallite size and lattice strain can be evaluated by plotting 2sinθ in x-direction and $\beta_{h\ k\ l}\cos\theta$ in y-direction, which is a linear fit. The intercept on the y-direction gives the size of the nanocrystals and the slope of the plot represents the average strain induced in the particles. According to this model, the average strain from the slope is found to be 0.93×10^{-3} and the average particle size is 88 nm. Here the graph shows a negative slope indicating a lattice shrinkage, which is observed from the calculation of lattice parameter, as well.

The Williamson-Hall plot of USDM is shown in Fig. 5. According to Hooke law, the stress and lattice strain is related by the equation $\sigma = Y_{h\ k\ l} \times \epsilon$, where σ is the stress, ε the lattice strain and $Y_{h\ k\ l}$ is the Young's modulus. Among these three models, the USDM and UDEDM are based on the anisotropic nature of the materials [42]. According to USDM, the modified Williamson-Hall equation is [44, 45]:

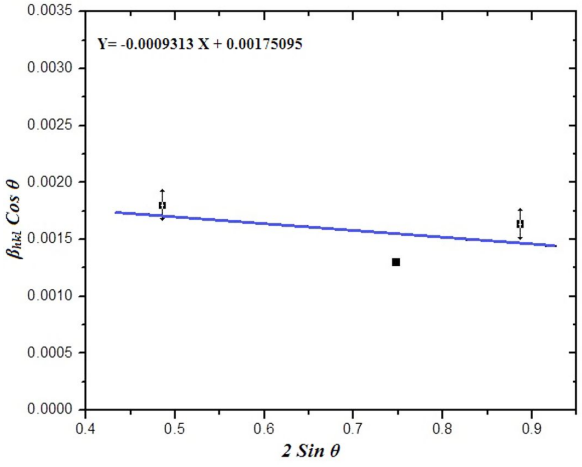

Fig. 4. Plot of $\beta_{h\ k\ l}\cos\theta$ vs. 2sinθ.

$$\beta_{hkl}\cos\theta = \frac{k\lambda}{D} + \frac{4\sigma\sin\theta}{Y_{hkl}} \tag{8}$$

In this equation, the lattice strain (ε) in the uniform deformation model is replaced by $\sigma/Y_{h\ k\ l}$, where $Y_{h\ k\ l}$ is the Young modulus in the perpendicular direction to (h k l) plane.

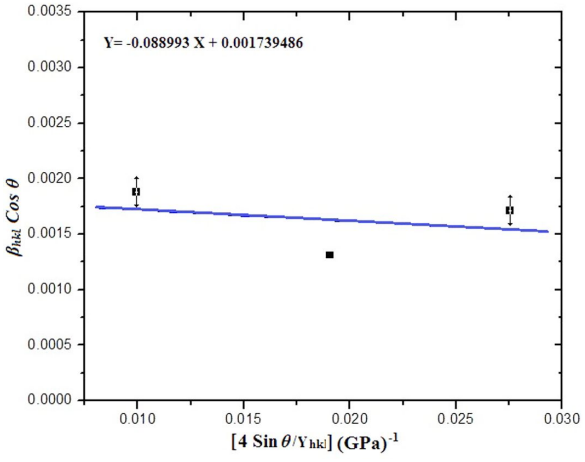

Fig. 5. Plot of $\beta_{h\ k\ l}\cos\theta$ vs. $\{(4\sin\theta)/Y_{h\ k\ l}\}$.

Plotting $4\sin\theta/Y_{h\,k\,l}$ in x-direction and $\beta_{h\,k\,l}\cos\theta$ in y-direction, the uniform stress as well as the lattice strain can be calculated from the slope.

The Young modulus ($Y_{h\,k\,l}$) for a cubic structure is given by [46–48]:

$$Y_{hkl} = 1/[S_{11} - 2\{(S_{11} - S_{12}) - 1/2(S_{44})\} \times (l^2m^2 + m^2n^2 + n^2l^2)] \quad (9)$$

where, S_{11}, S_{12} and S_{44} are the matrix components of the elastic compliances S and l, m, n are the direction cosines. The relationship between elastic compliances (S) and the stiffness constant (C) are given by equations 10, 11, 12:

$$S_{11} = \frac{(C_{11} + C_{12})}{[(C_{11} - C_{12})(C_{11} + 2C_{12})]} \quad (10)$$

$$S_{12} = \frac{(-C_{12})}{[(C_{11} - C_{12})(C_{11} + 2C_{12})]} \quad (11)$$

$$S_{44} = \frac{1}{C_{44}} \quad (12)$$

The values of stiffnes constants C_{11}, C_{12} and C_{44} for CdS nanocrystals are shown in Table 1 [49].

Using the values of stiffness constants C_{11}, C_{12} and C_{44} in equation 10, equation 11 and equation 12, the calculated value of elastic compliances of S_{11}, S_{12} and S_{44} are 0.020292×10^{-10}, -0.076×10^{-10}, and 0.2557×10^{-10}, respectively. From these values of compliances (S), the Young modulus in different directions can be easily calculated. The value of Young modulus in different directions is given in Table 2. Thus, the value of stress calculated from the slope is 88.99 MPa.

According to UDEDM, lattice strain is based on the energy density of deformation. According to the Hooke's law, $u = (\varepsilon^2 \times Y_{h\,k\,l})/2$, assuming uniform energy density (u) as a function of lattice strain (ε), then the modified Williamson-Hall equation can be written as:

$$\beta_{hkl}\cos\theta = \frac{k\lambda}{D} + \left\{4\sin\theta\sqrt{\frac{2u}{Y_{hkl}}}\right\} \quad (13)$$

The plot of uniform deformation energy density model is shown below in Fig. 6. The uniform energy density can be calculated from the slope by plotting $4\sin\theta\sqrt{\frac{2}{E_{hkl}}}$ in x-direction and $\beta_{h\,k\,l}\cos\theta$ in y-direction. Knowing the values of Young modulus ($Y_{h\,k\,l}$) of the sample, the lattice strain can be easily calculated. The stress and the energy density can be related to $u = \sigma^2/Y_{h\,k\,l}$, using equation 7 and equation 13. However, both the models USDM and UDEDM are different, as they are based on the assumption of uniform deformation stress and uniform deformation energy density as per equation 8 and equation 13. However, both the models (USDM and UDEDM) describe the crystalline anisotropic nature.

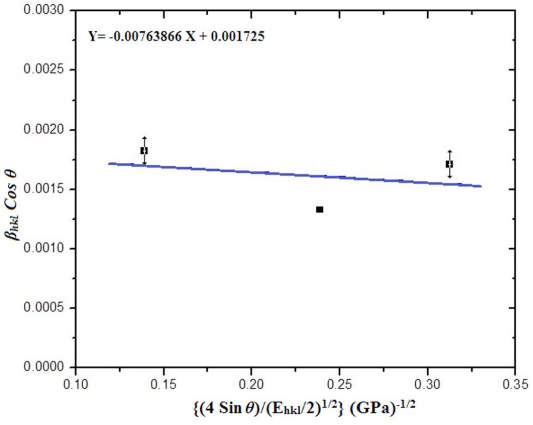

Fig. 6. Plot of $\beta_{h\,k\,l}\cos\theta$ vs. $\{(4\sin\theta)/Y_{h\,k\,l}/2)\}$.

3.2.4. Size-strain plot method

The W-H plot is based on isotropic nature of the XRD line broadening profile [36], which further reveals that the diffraction domains are isotropic [39]. Now, in the case of isotropic line broadening, the average "size-strain plot" (SSP) gives a far better size and strain parameters. This SSP method has an extra advantage that a less importance is given to the XRD data from all the reflections at higher angles. In this method it is also considered that crystallite size profile is a Lorentzian function and 'strain profile' is described by the Gaussian function [39, 41], which gives us:

$$(d_{hkl}\beta_{hkl}\cos\theta)^2 = \frac{k\lambda}{D}(d_{hkl}^2\beta_{hkl}\cos\theta) + \frac{\varepsilon^2}{4} \quad (14)$$

Table 1. Stiffness constant (C) values of cadmium sulfide (CdS).

Cadmium sulfide (CdS)			Anisotropy ratio
$C_{11} \times 10^{10}$ [N/m^2]	$C_{12} \times 10^{10}$ [N/m^2]	$C_{44} \times 10^{10}$ [N/m^2]	$(C_{11}-C_{12})/ C_{44}$
8.94	5.35	3.91	0.459

Table 2. Young modulus in different (h k l) planes.

Cadmium sulfide (CdS)		
Reflection planes	Young modulus of different planes	Values of Young modulus [GPa]
(1 1 1)	Y_{111}	97.83
(2 2 0)	Y_{220}	78.50
(3 1 1)	Y_{311}	64.31

where, k is the shape factor and $d_{h\,k\,l}$ is the lattice distance between the (h k l) planes calculated from the Bragg law. The SSP plot for CdS nanocrystals is obtained by plotting $(d^2_{h\,k\,l}\beta_{h\,k\,l}\cos\theta)$ in x-direction and $(d_{h\,k\,l}\beta_{h\,k\,l}\cos\theta)^2$ in y-direction for different peaks of XRD in the range of $2\theta = 20°$ to 60° as shown in Fig. 7. In this case, the particles size is obtained from the slope, and the root of the intercept in y-direction gives the strain value.

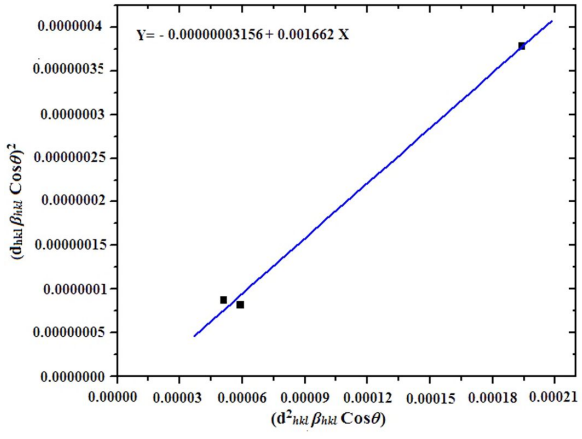

Fig. 7. Plot of $(d^2_{h\,k\,l}\beta_{h\,k\,l}\cos\theta)$ vs. $(d_{h\,k\,l}\beta_{h\,k\,l}\cos\theta)^2$.

The results obtained from the Scherrer method, different modified models of Williamson-Hall (W-H) equation (such as, UDM, USDM, and UDEDM), size-strain plot and the TEM analysis are summarized in Table 3. In this work, the lattice strain (ϵ) calculated from the modified W-H models and SSP method is found to be comparable with each other. The negative slope as obtained in W-H plot, actually results from the lattice shrinkage [39, 50, 51]. Moreover, the average value of crystalline size of the CdS nanocrystals obtained from different models is almost the same.

3.2.5. RMS strain estimation

The root-mean-square microstrain (ϵ_{rms}) is an important parameter and it can be obtained from the upper-limit microstrain considering the Gaussian strain distribution [52], whereas, Wilson method [53] has been used to calculate the upper-limit microstrain (ε_{hkl}). These are defined as:

$$\varepsilon_{hkl} = (\Delta d/d_0) \tag{15}$$

$$< \varepsilon_{RMS} >= (\frac{2}{\pi})^{1/2}(\Delta d/d_0) \tag{16}$$

In the above equation, Δd and d_0 are the observed and the ideal value of interplaner spacing in different $\langle$h k l$\rangle$ directions of the XRD peaks respectively. From the variation in the interplaner spacing, the estimated root-mean-square microstrain (ϵ_{rms}) values have been plotted against the upper-limit microstrain ($\epsilon_{h\,k\,l}$) as shown in Fig. 8. When the strain values agree, all these points must lie on a straight line making an angle of 45° with the x-axis [54, 55]. It is found from the plot that the RMS strain varies linearly with the strain calculated from the interplanar spacing [54]. The intercept of the graph gives the RMS strain value for

Table 3. Parameters of jagged spherical CdS nanocrystals calculated from different methods.

Sample name	TEM	Scherrer method		Williamson-Hall plot									SSP plot	
Jagged	Size	Size (D) [nm]		UDM		USDM			UDEDM				Size	$\epsilon\times 10^{-3}$
spherical	(D)	From	From	D	$\epsilon\times 10^{-3}$	D	$\epsilon\times 10^{-3}$	σ	D	$\epsilon\times 10^{-3}$	σ	U		
CdS	[nm]	equation	graph	[nm]	no unit	[mm]	no unit	[MPa]	[mm]	no unit	[MPa]	[KJ/m^3]	D [nm]	no unit
	100	81.10	93.74	88	0.93	88.61	0.90	88.99	89.33	1.03	75.55	58.34	92.71	0.355

the jagged spherical CdS which is 1.05×10^{-3}. All the values of strain calculated from the different models are less in comparison to the RMS value obtained.

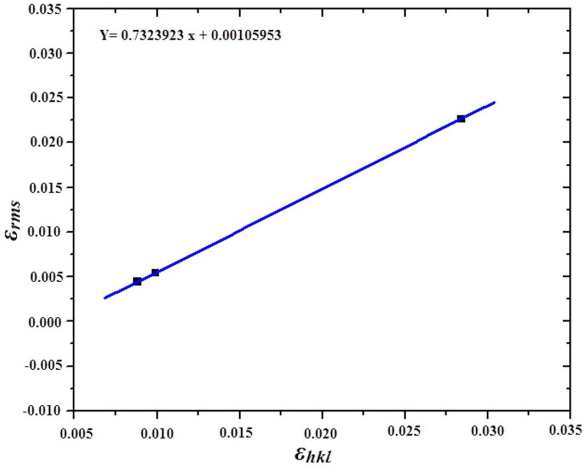

Fig. 8. Plot of ϵ_{rms} vs. $\epsilon_{\mathrm{h\,k\,l}}$.

4. Conclusion

Jagged spherical shaped CdS nanocrystals have been synthesized by chemical process and characterized by the X-ray diffraction (XRD) and high resolution transmission electron microscope (HRTEM). X-ray diffraction (XRD) study revealed that the nanocrystals are cubic in structure. The crystallite size was evaluated by the Scherrer method, Scherrer plot and modified form of Williamson-Hall equations, and it is in good agreement with the HRTEM analysis. The lattice strain was also calculated by the modified form of Williamson-Hall equations and size-strain plot. The graph for modified W-H plots showed a negative slope in the jagged spherical shaped CdS nanocrystals, which arose due to the lattice shrinkage. The results of the broadening analysis by W-H plots and SSP plot are in good intercorrelation with each other. HRTEM result also matches well with the results of Williamson-Hall methods, SSP method and RMS strain method.

Acknowledgements

The authors wish to thank the SAIF at the North-Eastern Hill University (NEHU), Shillong, for TEM micrograph and to Mr. Ratan Boruah, a Technical Asistant in the Department of Physics, Tezpur University, Assam (India), for the assistance during the X-ray diffraction analysis.

References

[1] Landes C.F., Link S., Babak Nikoobakht M.B.M., El-Sayed M.A., *Pure Appl. Chem.,* 74 (9) (2002), 1675.
[2] Pinna N., Weiss K., Urban J., Pileni M.P., *Adv. Mater.*, 13 (4) (2001), 261.
[3] Chae W.S., Shin H.W., Lee E.S., Shin E.J., Jung J.S., Kim Y.R., *J. Phys. Chem. B*, 109 (2005), 6204.
[4] Burda C., Chen X., Narayanan R., El-Sayed M.A., *Chem. Rev.*, 105 (2005), 1025.
[5] Manna L., Milliron D.J., Meisel A., Scher E.C., Alivisatos A.P., *Nature Mater.*, 2 (2003), 382.
[6] Cao H., Wang G., Zhang S., Zhang X., Rabinovich D., *Inorg. Chem.*, 45 (2006), 5103.
[7] Pandey G., Dixit S., *J. Phys. Chem. C*, 115 (2011), 17633.
[8] Garcia M.A., Merino J.M., Pinel E.F., Quesada A., Venta J. De la, Gonzalez M.L.R., Castro G.R., Crespo P., Llopis J., Gonza´lez-Calbet J.M., Hernando A., *Nano Lett.*, 7 (6) (2007), 1489.
[9] Tachikawa S., Noguchi A., Tsuge T., Hara M., Odawara O., Wada H., *Materials*, 4 (2011), 1132.
[10] Demir R., Gode F., *Chalcogenide Lett.*, 12 (2) (2015), 43.
[11] Borah J.P., Sarma K.C., *Acta Phys. Pol. A*, 114 (4) (2008), 713.
[12] Sharma M., Kumar S., Pandey O.P., *J. Nanopart. Res.*, 12 (2010), 2655.
[13] Bezdetko Y.S., Klyuev V.G., *Proc. Nap.*, 3 (2014), 01PCSI03.
[14] Hao E., Anderson N.A., Asbury J.B., Lian T., *J. Phys. Chem. B*, 106 (2002), 10191.

[15] AMELIA M., FLAMINI R., LATTERINI L., *Langmuir*, 26 (12) (2010), 10129.
[16] MURAKOSHI K., HOSOKAWA H., SAITOH M., WADA Y., SAKATA T., MORI H., SATOH M., YANAGIDA S., *J. Chem. Soc. Faraday T.,* 94 (4) (1998), 579.
[17] BANERJEE R., JAYAKRISHNAN R., AYYUB P., *J. Phys.: Condens. Mater.*, 12 (2000), 10647.
[18] LI L., YANG X., GAO J., TIAN H., ZHAO J., HAGFELDT A., SUN L., *J. Am. Chem. Soc.*, 133 (2011), 8458.
[19] DEMIR R., OKUR S., ŞEKER M., *Indian Eng. Chem. Res.*, 51 (2012), 3309.
[20] QIAN J., YAN S., XIAO Z., *J. Colloid Interf. Sci.*, 366 (2012), 130.
[21] MARTÍNEZ-ALONSO C., RODRÍGUEZ-CASTAÑEDA C.A., MORENO-ROMERO P., CORIA-MONROY C.S., HU H., *Int. J. Photoenergy*, 2014 (2014), 453747.
[22] KUMAR L., DHAWAN S.K., KUMAR M., KAMALASANAN M.N., CHANDRA S., *IJPAP*, 41 (2003), 641.
[23] SUN W., ZHONG J., ZHANG B., JIAO K., *Anal. Bioanal. Chem.*, 389 (2007), 2179.
[24] GONÇALVES L.F.F.F., KANODARWALA F.K., STRIDE J.A., SILVA C.J.R., GOMES M.J.M., *Opt. Mater.*, 36 (2013), 186.
[25] RAJ F.M., RAJENDRAN A.J., *Int. J. Innov. Res. Sci. Eng. Tech.*, 4 (1) (2015), 56.
[26] IKHMAYIES S.J., *Int. J. Mater. Chem.*, 3(2) (2013), 28.
[27] URBIOLA I.R.C., MARTÍNEZ J.A.B., BORJA J.H., GARCÍA C.E P., BON R.R., VOROBIEV Y.V., *Energy Proc.*, 57 (2014), 24.
[28] SUN S.Q., LI T., *Cryst. Growth Des.*, 7 (11) (2007), 2367.
[29] QI W.H., WANG M.P., XU G.Y., *J. Mater. Sci. Lett.*, 22 (2003), 1333.
[30] QI W.H., WANG M.P., *J. Nanoparticle Res.*, 7 (2005), 51.
[31] UNGAR T., *J. Mater. Sci.*, 42 (2007), 1584.
[32] CULLITY B.D., DENNIS B., *Elements of X-ray diffraction*, 2^{nd} ed., Addision-Wesley Publishing Company Inc., 1978.
[33] CHANDEL S., ANJAN P.R., VALLAMATTOM A.J., NAMPOORI V.P.N., RADHAKRISHNAN P., *International Conference on Fiber Optics and Photonics*, OSA 2012.
[34] DEY P.C., DAS R., *J. Lumin.*, 183 (2017), 368.
[35] UVAROV V., POPOV I., *Mater. Charact.*, 58 (2007), 883.
[36] DAS R., SARKAR S., *Opt. Mater.*, 48 (2015), 203.
[37] DAS R., SARKAR S., *Curr. Sci.*, 109 (4) (2015), 775.
[38] DAS R., NATH S.S., BHATTACHARJEE R., *Physica E*, 43 (1) (2010), 224.
[39] ZAK A.K., MAJID W.H.ABD., ABRISHAMI M.E., YOUSEFI R., *Solid State Sci.*, 13 (2011), 251.
[40] PRABHU Y.T., RAO K.V., SAI KUMAR V.S., KUMARI B.S., *World J. Nano Sci. Eng.*, 4 (2014), 21.
[41] JACOB R., ISAC J., *Int. J. Chem. Studies*, 2 (5) (2015), 12.
[42] SENTHIL SARAVANAN M.S., SIVAPRASAD K., SUSILA P., KUMARESH BABU S.P., *Physica B*, 406 (2011), 165.
[43] BIRKHOLZ M., *Thin film analysis by X-ray scattering*, Wiley-VCH Verlag GmbH and Co., KGaA, Weinheim, 2006.
[44] VENKATESWARLU K., BOSE A.C., RAMESHBABU N., *Physica B*, 405 (20) (2010), 4256.
[45] SIVAKAMI R., DHANUSKODI S., KARVEMBU R., *Spectrochim. Acta Part A*, 152 (2016), 43.
[46] YAN Z., VINCENT J., *Sci. China-Phys. Mech. Astron.*, 56 (4) (2013), 694.
[47] LALENA J.N., CLEARY D.A., *Principles of Inorganic Materials Design*, 2^{nd} ed., John Wiley & Sons, Inc. Publication, Hoboken, New Jersey, 2010.
[48] CAZZANI A., ROVATI M., *Int. J. Solids Struct.*, 40 (2003), 1713.
[49] WRIGHT K., GALE J.D., *Phys. Rev. B*, 70 (2004), 035211.
[50] VAEZI M.R., SHAH GHASSEMI S.H.M., SHOKUHFAR A., *Mater. Sci.-Poland*, 26 (3) (2008), 601.
[51] BHUSHAN B., LUO D., SCHRICKER S.R., SIGMUND W., ZAUSCHER S., *Handbook of nanomaterials properties*, Springer Heidelberg, New York – Dordrecht – London, 2014.
[52] ORTIZ A.L., SHAW L., *Acta Mater.*, 52 (2004), 2185.
[53] WILSON, A.C.J., *X-ray Optics*, London, 1949.
[54] BIJU V., SUGATHAN N., VRINDA V., SALINI S.L., *J. Mater. Sci.*, 43 (2008), 1175.
[55] BINDU P., THOMAS S., *J. Theor. Appl. Phys.*, 8 (2014), 123.

Received 2017-06-09
Accepted 2019-04-23